ELSEVIER

Desalination 212 (2007) 261–281

DESALINATION

www.elsevier.com/locate/desal

A mini-review of modeling studies on membrane bioreactor (MBR) treatment for municipal wastewaters

Aileen N.L. Ng, Albert S. Kim*

Civil and Environmental Engineering, University of Hawaii at Manoa,
2540 Dole Street Holmes 383, Honolulu, HI 96822, USA
Tel. +1 (808) 956-3718; Fax +1 (808) 956-5014; email: AlbertSK@hawaii.edu

Received 3 July 2006; accepted 19 October 2006

Abstract

Membrane bioreactor (MBR) technology is a promising method for water and wastewater treatment because of its ability to produce high-quality effluent that meets water quality regulations. Due to the intrinsic complexity and uncertainty of MBR processes, basic models that can provide a holistic understanding of the technology at a fundamental level are of great necessity. Compared to experimental research and development, followed by commercialization of the technology, modeling studies for system design analysis and performance prediction are at a relatively rudimentary state. In this light, this review was conducted to provide an assessment of present efforts in modeling MBR systems, specifically for municipal wastewater treatment. Models considered in this review are classified into three categories: biomass kinetic models, membrane fouling models, and integrated models with (light) couplings to describe the complete MBR process. The specific features, unique advantages, and capturing capability of experimental observations of each model are discussed and assessed. Crucial components in MBR modeling studies are carefully selected and assessed, based on the importance of their roles in characterizing MBR performance, and future MBR modeling directions are suggested.

Keywords: Membrane bioreactor (MBR); Wastewater treatment; Activated sludge models; Membrane fouling

1. Introduction

The membrane bioreactor (MBR) is a system that combines biological treatment with membrane filtration into a single process. The first reported application of MBR technology was in 1969, when an ultrafiltration membrane was used to separate activated sludge from the final effluent of a biological wastewater treatment system and the sludge was recycled back into the aeration tank [1]. Since then, the MBR system has evolved, and research on MBR technology has increased significantly, particularly in the last 5 years [2].

*Corresponding author.

Two basic MBR configurations are shown in Fig. 1 (modified from [3]). The first is a recirculated configuration with an external membrane unit (Fig. 1a). Mixed liquor is circulated outside of the reactor to the membrane module, where pressure drives the separation of water from the sludge. The concentrated sludge is then recylced back into the reactor. The second is a submerged configuration with the membrane module immersed in the activated sludge (Fig. 1b). A suction force is applied to draw the water through the membrane, while the sludge is retained on the membrane surface. A manifold at the base of the reactor diffuses compressed air within the reactor, providing oxygen to maintain aerobic conditions. The air bubbles also function to scour the membrane surface and clean the exterior of the membrane as they rise in the reactor. The submerged configuration is more commonly used than the recirculated configuration because it is less energy-intensive and provides a cleaning mechanism to reduce membrane fouling. Thus, more fouling models focus on the submerged configuration than on the external configuration.

There are many applications for the MBR system. In general, the applications can be grouped into three categories of processes involving water filtration membranes, gas diffusion membranes, and extractive membranes (including ion exchange). In the last 15 years, research on MBR applications for water and wastewater treatment has been predominant, while research on MBR applications for the other two areas has received less attention [2].

The advantages of the MBR system over conventional biological treatment processes spur the growing interest in MBR technology for water and wastewater treatment. MBR treatment of municipal wastewater yields high-quality water with reported removal percentages of 95%, 98%, and 99% (or greater) for chemical oxygen demand (COD), biochemical oxygen demand (BOD), and suspended solids (SS), respectively [4]. This is important as water quality regulations have become increasingly stringent. A MBR has greater (independent) control over the suspended solids retention time (SRT) and hydraulic retention time (HRT) because membrane filtration rather than gravitational settling is used to separate the biomass from the effluent. This allows for operation at a longer SRT and at higher loading rates, which results in less sludge production and shortens the necessary HRT. The use of membranes to separate the biomass from the effluent also eliminates the need for large clarifying basins to settle out the biomass, thus enabling the system to be more compact.

Models that can accurately describe the MBR process are valuable for the design, prediction, and control of MBR systems. Complex models

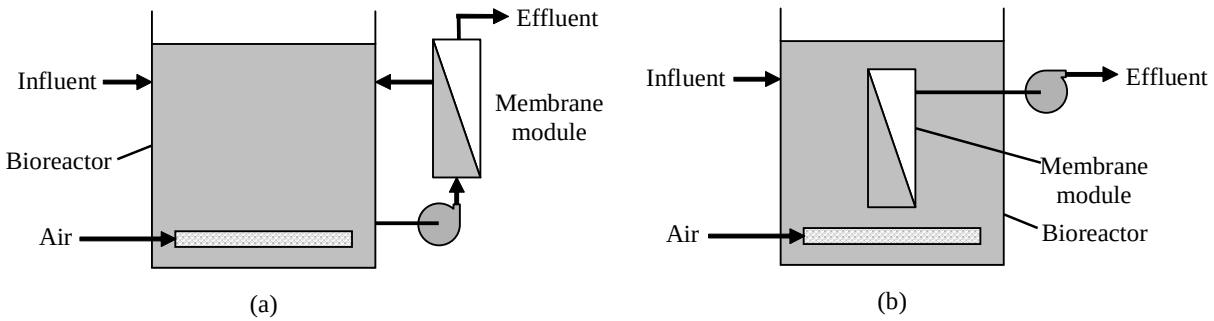

Fig. 1. Schematic diagrams of basic membrane bioreactor configurations [3]: (a) MBR with external membrane module and (b) MBR with immersed membrane module.

that are also practical for real applications can greatly assist in capitalizing on the benefits of MBR technology. This review of published works on MBR process modeling for treatment of municipal wastewaters is classified into biomass kinetics models, membrane fouling models, and integrated models (that combine biomass kinetics and membrane fouling models to describe the complete MBR system).

2. MBR model description and assessment

2.1. Biomass kinetic models

2.1.1. The activated sludge model (ASM) family

In 1983, the International Association on Water Pollution Research and Control, later known as the International Association on Water Quality and now the International Water Association (IWA), formed a task group to develop a practical model for the design and operation of the biological wastewater treatment process. The product of the group's efforts is activated sludge model no. 1 [5], introduced in 1987. Versions that expanded and improved upon the first model were introduced by the association in later years. They include activated sludge model no. 2 [6], which incorporates phosphorus removal from wastewaters; activated sludge model no. 2d [7], which accounts for the ability of phosphorus-accumulating organisms to use cell internal substrates for denitrification; and activated sludge model no. 3 [8], which does not include phosphorus removal but addresses problems found in the first model.

Although the ASMs were developed to describe the conventional activated sludge process, it has been suggested that the models can also be used to simulate biomass kinetics in an MBR system [9–11]. The MBR process is the activated sludge process with the secondary clarification step replaced by membrane filtration; therefore, it is reasonable to use ASMs to characterize the biomass dynamics in an MBR system. Presented here is a brief overview of the four ASMs. The IWA task group publication [12] should be referred to for further details on the models' components, processes, calibration methods, applications, and limitations.

2.1.1.1. Activated sludge model no. 1 (ASM1)

Activated sludge model no. 1 was developed to model biological treatment for organic carbon removal, nitrification, and denitrification. The model can be used to predict oxygen demand and sludge production in an activated sludge system. Two main concepts have been incorporated into the model. The first concept is that biodegradable COD in wastewater is composed of readily biodegradable COD (RDCOD) and slowly biodegradable COD (SBCOD). RBCOD can immediately be used by organisms for synthesis, whereas SBCOD must be broken down before it can pass through the organisms' cell wall to be metabolized. Total COD in the model is comprised of biodegradable COD, non-biodegradable COD (i.e., inert material), and the active biomass. The second concept in this model is death-regeneration. When the biomass decays, a portion of the decayed cell material is non-biodegradable and remains inert. The rest of the decayed material is slowly biodegradable and can be broken down to be used by active organisms for growth.

Fig. 2 shows the main processes included in ASM1, i.e., the hydrolysis of slowly biodegradable material and the growth and decay of the organisms in the biomass. Two groups of organisms considered in the model are autotrophs ($X_{B,A}$) and heterotrophs ($X_{B,H}$). Autotrophs perform the nitrifying activities. Their growth occurs through the oxidation of ammonia (S_{NH}) to nitrate (S_{NO}), which transpires only under aerobic conditions. This process is modeled using saturation-type (Monod) kinetics. Heterotrophs perform the carbon removal and denitrifying activities. They consume soluble substrate (S_S), which includes readily biodegradable decayed cell material, and ammonia for

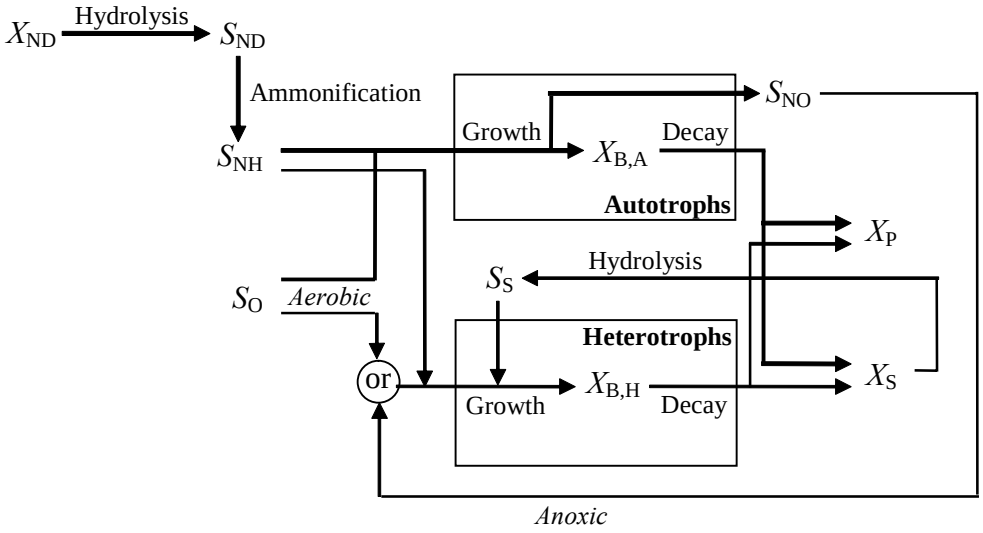

Fig. 2. Diagram of model processes and substrate flow in ASM1.

growth under both aerobic and anoxic conditions. Under aerobic conditions, oxygen is utilized in the growth process. Under anoxic conditions, when oxygen is absent, nitrate is used as the electron acceptor and is reduced to dinitrogen. The heterotrophic growth process is likewise modeled using saturation-type kinetics. The decay processes for both types of organisms are described by the death-regeneration concept with first-order kinetics. However, only heterotrophs can reuse the biodegradable decay material for growth, and the autotrophic decay rate is relatively slower.

The basic structure of ASM1 is a mass balance equation to describe the accumulation rate of a particular component within the system:

Accumulation = Input – Output + Reaction

The model supplies reaction rate expressions for the various model components, so that they can be applied to many different process configurations. A matrix format is used to allow easy identification of the rate processes that affect the fate of each component. A partial section of the ASM1 matrix is shown in Table 1. The reaction rate *r* of a component, *i*, can be read from the matrix by traversing down column *i* and adding the products of the coefficient ν_{ij} and the corresponding process rate ρ_j, i.e.,

$$r_i = \sum_j \nu_{ij} \rho_j \tag{1}$$

If no coefficient is listed in the table, the coefficient is assumed to be zero. To demonstrate, the reaction rate for autotrophic biomass, $X_{B,A}$, is

$$r_{X_{B,A}} = 1 \cdot \hat{\mu}_A \left(\frac{S_{NH}}{K_{NH} + S_{NH}} \right) \left(\frac{S_O}{K_{O,A} + S_O} \right) X_{B,A} + (-1) \cdot b_A X_{B,A} \tag{2}$$

and the reaction rate for particulates arising from biomass decay, X_p, is

$$r_{X_p} = f_p \cdot b_H X_{B,H} + f_p \cdot b_A X_{B,A} \tag{3}$$

In the model, $\mu_?$ denotes a maximum growth rate, $K_?$ is a saturation coefficient, and $b_?$ is a rate constant. Thirteen components are incorporated

Table 1
A partial section of the matrix of process kinetics and stoichiometry from ASM1

Component i		6	7	8	Process rate, ρ_j
j	Process	$X_{B,A}$	X_P	S_O	[M/L^3/T]
1	Aerobic growth of heterotrophs			$-\frac{1-Y_H}{Y_H}$	$\hat{\mu}_H\left(\frac{S_S}{K_S+S_S}\right)\left(\frac{S_O}{K_{O,H}+S_O}\right)X_{B,H}$
3	Aerobic growth of autotrophs	1		$-\frac{4.57-Y_A}{Y_A}$	$\hat{\mu}_A\left(\frac{S_{NH}}{K_{NH}+S_{NH}}\right)\left(\frac{S_O}{K_{O,A}+S_O}\right)X_{B,A}$
4	Decay of heterotrophs		f_P		$b_H X_{B,H}$
5	Decay of autotrophs	–1	f_P		$b_A X_{B,A}$

in the model, and a mass balance equation can be derived for each of these components from the eight rate processes listed in Table 2. The inert materials, X_I and S_I, are incorporated in the model despite having a zero reaction rate. Particulate inert material, X_I, becomes enmeshed in the activated sludge and is removed from the system through sludge waste. Soluble inert material, S_I, leaves the system at the same concentration with which it enters. All organic material and biomass components are expressed in terms of COD because it can be used to link organic substrates, biomass, and consumed oxygen by electron equivalents. Likewise, oxygen is expressed as negative oxygen demand.

A number of simple assumptions made in the model impose limitations on its application. One assumption is that the system operates at a constant temperature. However, the thermal sensitivity of the model parameters can be incorporated in the rate expressions by applying the Arrhenius equation. Another assumption is that the system operates at a constant pH near neutral. Although it is known that pH can influence some model parameters, few expressions exist to capture this influence. Therefore, alkalinity has been included in the model to allow detection of problems with pH control. The model parameters in the rate expression are assumed to be constant. Consequently, the model does not handle changes in wastewater characteristics. The effects of low nutrient concentrations (e.g., phosphorous, nitrogen, and other inorganic nutrients) on the removal of organic substrate and cell growth are not specifically considered. It is presumed that sufficient quantities of nutrients are present to allow for balanced growth of organisms. Although the biomass may change in species diversity over time, the kinetic parameters remain fixed in the model as it would be too complicated to capture such an effect on the kinetic parameters. Other assumptions made in the model include a constant value for nitrification-related parameters, which are presumed to incorporate inhibitory effects of waste constituents, instantaneous entrapment of particulate organics by the biomass, coupled and simultaneous occurrence of the hydrolysis of organic matter and organic nitrogen at equal rates, and indifference of the electron acceptor type on biomass decay.

Table 2
Components and rate processes in ASM1, ASM2, and ASM3

	Components	Processes
ASM1	Soluble inert organic matter (S_I)	Aerobic growth of $X_{B,H}$
	Readily biodegradable substrate (S_S)	Anoxic growth of $X_{B,H}$
	Particulate (suspended) inert organic matter (X_I)	Aerobic growth of $X_{B,A}$
	Slowly biodegradable substrate (X_S)	Decay of $X_{B,H}$
	Active heterotrophic biomass ($X_{B,H}$)	Decay of $X_{B,A}$
	Active autotrophic biomass ($X_{B,A}$)	Ammonification of S_{ND}
	Particulates arising from biomass decay (X_P)	Hydrolysis of entrapped organics
	Oxygen (negative COD) (S_O)	Hydrolysis of entrapped organic nitrogen
	Nitrate and nitrite nitrogen (S_{NO})	
	Ammonia and ammonium nitrogen (S_{NH})	
	Soluble biodegradable organic nitrogen (S_{ND})	
	Particulate biodegradable organic nitrogen (X_{ND})	
	Alkalinity (S_{ALK})	
ASM2	Dissolved oxygen (S_{O_2})	Aerbobic hydrolysis
	Fermentable (readily biodegradable substrate (S_F)	Anoxic hydrolysis
	Fermentation products (S_A)	Anaerobic hydrolysis
	Ammonium and ammonia nitrogen (S_{NH_4})	Aerobic growth of X_H on S_F
	Nitrate and nitrite nitrogen (S_{NO_3})	Aerobic growth of X_H on S_A
	Inorganic soluble phosphorus (S_{PO_4})	Anoxic growth of X_H on S_F
	Inert soluble organic material (S_I)	Anoxic growth of X_H on S_A
	Alkalinity (S_{ALK})	Fermentation
	Dinitrogen (S_{N_2})	Lysis of X_H
	Inert particulate organics (X_I)	Storage of X_{PHA}
	Slowly biodegradable substrates (X_S)	Storage of X_{PP}
	Heterotrophic organisms (X_H)	Aerobic growth of X_{PAO} on X_{PHA}
	Phosphate accumulating organisms (X_{PAO})	Lysis of X_{PAO}
	Polyphosphates (X_{PP})	Lysis of X_{PP}
	Cell internal storage products of PAO (X_{PHA})	Lysis of X_{PHA}
	Nitrifing organisms (X_{AUT})	Aerobic growth of X_{AUT}
	Total suspended solids (X_{TSS})	Lysis of X_{AUT}
	Metal hydroxides (X_{MeOH})	Precipitation of S_{PO_4}
	Metalphosphate (X_{MeP})	Redissolution of S_{PO_4}
ASM3	Dissolved oxygen (negative COD) (S_O)	Hydrolysis
	Inert soluble organic matter (S_I)	Aerobic storage of S_S
	Readily biodegradable organic substrate (S_S)	Anoxic storage of S_S
	Ammonium plus ammonia nitrogen (S_{NH_4})	Aerobic growth of X_H
	Dinitrogen (S_{N_2})	Anoxic growth of X_H
	Nitrate and nitrite nitrogen (S_{NOX})	Aerobic endogenous respiration of X_H
	Alkalinity (S_{ALK})	Anoxic endogenous respiration of X_H
	Inert particulate (suspended) organic matter (X_I)	Aerobic endogenous respiration of X_{STO}
	Slowly biodegradable substrate (X_S)	Aerobic endogenous respiration of X_{STO}
	Active heterotrophic organisms (X_H)	Aerobic growth of X_A
	Cell internal storage product of heterotrophic organisms (X_{STO})	Aerobic endogenous respiration of X_A
	Nitrifying organisms (X_A)	Anoxic endogenous respiration of X_A
	Suspended solids (X_{SS})	

2.1.1.2. Activated sludge model no. 2 (ASM2)

Activated sludge model no. 2, presented in 1995, expands upon ASM1 by including biological phosphorous removal. The model incorporates a new group of organisms to the biomass, which originally consisted of heterotrophs and autotrophs. The new group, called phosphorus-accumulating organisms (PAOs), encompasses the different types of microorganisms capable of accumulating phosphorous and storing them in the form of cell internal polyphosphates (X_{PP}) and poly-hydroxyalkanoates (X_{PHA}). PAOs are assumed to be incapable of denitrifying activity and can only grow on stored cell internal organic material X_{PHA}. Fig. 3 shows the storage and growth processes of PAOs in ASM2. PAOs store external fermentation products (S_A) in the form of internal cell storage material X_{PHA}. This process occurs primarily under anaerobic conditions, although it has been reported to occur under aerobic and anoxic conditions as well. For this reason, the kinetic expression for the storage of X_{PHA} does not include inhibition terms for dissolved oxygen and nitrate plus nitrite nitrogen. Energy for the process comes from the hydrolysis of X_{PP}, which leads to the release of soluble phosphates (S_{PO_4}). PAOs also store phosphates in the form of X_{PP} with the energy supplied from the respiration of X_{PHA}. X_{PP} is regenerated because PAOs require S_A stored in the form of X_{PHA} for growth, and the storage of S_A requires the energy from the hydrolysis of X_{PP}. According to the model, growth of PAOs occurs only under aerobic conditions at the expense of X_{PHA} and involves the consumption of S_{PO_4} and lysis of X_{PP}. Separate process rates are provided in the model for the lyses of PAOs and each of the two storage products to capture all losses of biomass due to respiration and maintenance or death.

In ASM2, the growth of heterotrophic organisms occurs under both aerobic and anoxic conditions from the consumption of both fermentable substrates (S_F) and fermentation products (S_A), thus involving four separate growth processes. The growth rates (μ_m) and yield coefficients (Y_H) are assumed to be identical regardless of the organic substrate (S_F or S_A) consumed. Under aerobic conditions, heterotrophic growth processes consume oxygen (S_{O_2}) and nutrients (S_{NH_4} and S_{PO_4}), and possibly alkalinity (S_{ALK}) to produce suspended solids (X_{TSS}). The anoxic growth processes utilize nitrate (S_{NO_3}) instead of oxygen, and the nitrate is reduced to dinitrogen (S_{N_2}). Denitrification, which releases alkalinity, is assumed to be inhibited by the presence of S_{O_2}, and the maximum growth rate is reduced to a fraction of that under aerobic conditions. The slower growth rate accounts for the fact that not all heterotrophs are capable of performing denitrification reactions. Under anaerobic conditions, when both oxygen and nitrate are not available, fermentation is assumed to occur. In this process, S_F is directly transformed by heterotrophs to S_A, and alkalinity is required due to the release of negatively charged

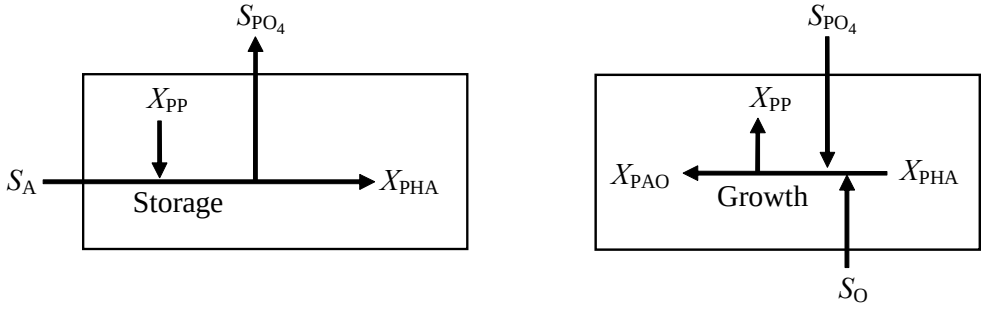

Fig. 3. Storage and growth processes involving PAO in ASM2 (modified from [2]).

S_A. Aside from rate limitations imposed by phosphate concentrations that are incorporated into the rate expression for autotrophic growth, processes involving autotrophic organisms are the same as in ASM1.

Two additional rate processes (precipitation and redissolution of phosphates) and two components (metalhydroxides and metal phosphates) were included in ASM2 to capture effects of the precipitation and redissolution of phosphates. Metals are naturally present in wastewater and can precipitate with soluble ortho-phosphates if both constituents exist in high enough concentrations. Also, it is common practice to add iron or alum salts to aid in phosphorous removal through chemical precipitation in conventional treatment processes. Table 2 lists the 19 components and 19 rate processes in the ASM2 model. The same model limitations of ASM1 apply to ASM2. Further assumptions and restrictions of ASM2 include the following. The heterotrophic and phosphate-accumulating biomasses are spatially homogenous and time-invariant. The internal structure of each individual cell is not distinguished, and only an average composition is considered despite the use of nonlinear kinetic expressions. A pragmatic decision was made to accept the problems associated with the use of average biomass compositions, as the introduction of population models would pose additional problems. The hydrolysis of organic matter, organic nitrogen, and organic phosphates is assumed to occur simultaneously in a coupled manner, and X_S comprises a constant fraction of nitrogen and phosphorous. This is a simplified assumption to avoid the addition of six more hydrolysis processes and two particulate components. Denitrification reactions of PAOs are not included in the model, although it is known that some PAOs can denitrify. Therefore, the model should be used only to simulate processes with low nitrate input into anaerobic tanks. The model assumes sufficient concentrations of phosphate, ammonia, potassium, and magnesium. The detailed mechanisms of growth limitations from low nutrient concentrations are not known and may not be accurately modeled. The effects of low potassium and magnesium concentrations on biological phosphorus removal are not considered. Finally, although nitrate and nitrogen monoxide have been observed to inhibit biological phosphorus removal, such effects are not incorporated in the model. In this review only critical assumptions that greatly affect model performance are highlighted. Other assumptions made in ASM2 are detailed in the IWA publication [12].

2.1.1.3. Activated sludge model no. 2d (ASM2d)

Activated sludge model no. 2d incorporates the observation that PAOs can use internal cell organic storage products for denitrification and thus grow under anoxic conditions. This observation led to the addition of two rate processes: the storage of polyphosphates and growth of PAOs under anoxic conditions. All other details of ASM2 carry over to ASM2d.

2.1.1.4. Activated sludge model no.3 (ASM3)

In 1999, the IWA task group revised ASM1 to produce a more accurate and updated model, ASM3. One of the major changes is the inclusion of internal cell storage compounds in heterotrophs, shifting the focus from hydrolysis to the storage of organic substrates. All readily biodegradable substrates are taken up by the heterotrophic biomass and stored as internal cell components prior to growth. Thus, heterotrophic growth is not fully dependent upon external compounds. The inclusion of internal cell storage structures also leads to the distinction between the decay of biomass and storage products under both aerobic and anoxic conditions. Another significant difference is the replacement of the death-regeneration concept by the growth-endogenous respiration model. In ASM1, the decay of organisms occurs at a certain rate, and a portion of the decayed cell material returns to the heterotrophic growth process.

In ASM3, endogenous respiration is used to capture all forms of biomass loss and energy requirements and is not associated with growth. The growth and decay of the two groups of organisms are clearly distinguished, as shown in Fig. 4, and identical models are used to describe the decay processes. These changes better reflect observed phenomena.

Components in ASM1 not included in ASM3, are particulates from biomass decay as well as soluble and particulate biodegradable organic nitrogen. Components added in ASM3 are dinitrogen, internal cell storage product of heterotrophic organisms, and suspended solids. The 13 components and 12 rate processes described in ASM3 are listed in Table 2. Limitations of the model are as follows. The model was developed for domestic wastewater and, therefore, should not be used to model industrial water treatment. It is applicable within the temperature range of 8–23ºC and a pH range of 6.5–7.5, excluding anaerobic conditions. The model is designed for systems only with low loads and high SRT (> 1 d) and is limited to low concentrations of nitrite.

2.1.1.5. Assessment of activated sludge models

ASM1 was tested extensively against experimental and operational data for activated sludge systems. Main problems found with ASM1 were addressed in the development of ASM3. ASM2, ASM2d, and ASM3 were also validated against experimental data for conventional activated sludge systems, although less extensively. It has been suggested that ASMs may be suitable for characterizing biomass kinetics in an MBR system. However, few studies have demonstrated the validity (or invalidity) of ASMs for modeling MBR systems.

In a study that introduces an integrated MBR model, Wintgens et al. [11] compare simulation results from ASM3 under steady-state conditions with mean measured values for COD, ammonium, and nitrate plus nitrite from a full-scale operational MBR plant. The simulation results corresponded well with the measured data. Although the study implies that ASM3 is a good modeling method for MBR systems, further in-depth studies are necessary to consider its accuracy for capturing other components and modeling transient states.

The applicability of ASMs for modeling MBR systems needs to be verified to further understand the effects of higher SRTs and mixed liquor suspended solids (MLSS) concentrations on biomass. Additionally, studies comparing the conventional activated sludge process with the MBR process can aid in understanding the effects of filtration versus clarification and estimating the potential capability of ASMs to capture such effects [13]. An advantage of using the ASMs is the clear

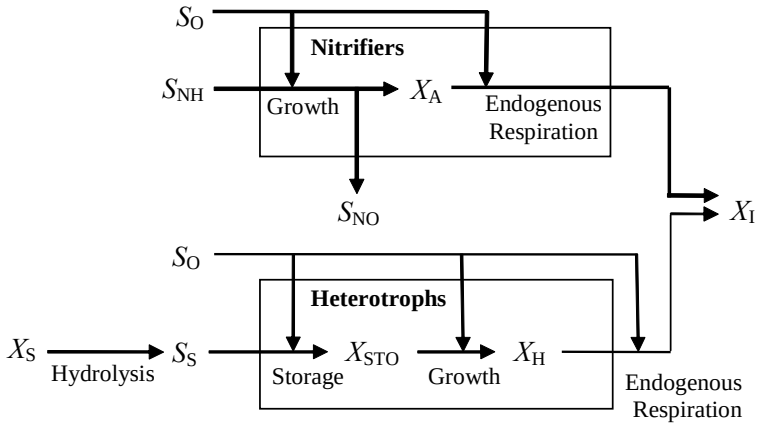

Fig. 4. Diagram of substrate in ASM3 (modified from [8]).

presentation in a matrix format. The matrix aids the understanding of the biological treatment process and the devising of efficient experimental design. Another advantage is that many simulation programs include ASMs or models based on ASMs, providing easy access of the models for various applications. Also, biological phosphorous removal, which is a key feature in biological treatment, is already incorporated into ASM2 and ASM2d.

2.1.2. Soluble microbial products (SMP) model

While there are nuances among researchers as to what comprises soluble microbial products (SMP), SMP are generally defined as *the organic materials arising from substrate metabolisms (usually with biomass growth) and biomass decay and being present in the effluent of biological systems but absent from the influent* [14]. Studies have shown that SMPs comprise a considerable portion of soluble organic matter in the effluent of biological treatment processes, and the presence of SMPs in the permeate is detrimental to the MBR process as well as to post-treatment processes [14]. While it is still unclear whether the accumulation of SMPs in the activated sludge inhibits metabolic activity, as contradicting results have been reported [15,16], studies agree that buildup of SMPs can cause reduction in membrane permeability [15–19]. Additionally, SMPs in the permeate stream can lead to formation of trihalomethanes and other disinfection by-products and cause bacterial growth in distribution systems [20]. Therefore, it is crucial to include SMPs in the modeling of biological water treatment processes.

In 1992, Furumai and Rittmann [20] presented a model that describes the interaction between heterotrophic and nitrifying bacteria in biological treatment processes. The model accounts for the formation and exchange of SMPs between heterotrophs and nitrifiers, which are known to compete with each other for dissolved oxygen. Nitrifiers can also supply potential energy for heterotrophs. They chemically reduce inorganic carbon to organic carbon in the form of cell mass and SMPs and make organic substrates available for growth of heterotrophs.

In the model, SMPs are divided into two groups: utilization-associated products (UAPs), which are produced by biomass growth, and biomass-associated products (BAPs), which arise from biomass decay. The two types of SMP are grouped together in the model, but their formation is accounted for separately. The formation rate of UAPs is proportional to the substrate utilization rate, whereas the formation rate of BAPs is proportional to the amount of active biomass. Both organisms produce SMPs, but only heterotrophs degrade them for cell synthesis. A mass balance equation of the system is provided for each of the model components (i.e., organic COD, ammonium, nitrite, dissolved oxygen, nitrate, originally formed SMP, actual SMP, heterotrophs, ammonium oxidizers, nitrite oxidizers, and inert biomass).

This model was modified in 1998 to include features specific to the MBR process [21,22]. Mainly, the output of biomass in the effluent was eliminated because the membranes retain the biomass in the system. The retention of a BAP fraction was considered in the same way because fractions of larger macromolecules are maintained in the reactor by membranes. Additionally, denitrification reactions were integrated into the model, and the biodegradation rates of the two types of SMP were modified according to recent findings, which suggested separate consumption rates for UAP and BAP using Monod-type kinetics. The model includes 10 transient mass balance equations to characterize each constituent considered in the model: heterotrophs, nitrifiers, inert biomass, soluble COD, ammonia, nitrate, nitrogen gas, oxygen, BAP, and UAP. As in ASMs, the multiplicative Monod equations were used to capture rate limitations stemming from the deficiency of necessary substrates.

The SMP model demonstrated good correspondence between simulation results and measured data. In a study conducted by Urbain et al. [21], a comparison was made between data from an MBR pilot plant and model predictions for oxygen demand, nutrient removal, sludge production, and biomass distribution under both steady and transient states at three different sludge ages. The model was not calibrated specifically for the pilot plant. Despite the use of default parameter values from published works, good correspondence was found between model predictions and experimental values for volatile suspended solids (VSS) concentration, effluent COD, and nitrogen species. The model demonstrated the capability of producing accurate predictions under both steady-state and transient-state cases. However, the SMP model could not handle technical problems during operation and sudden changes in the wastewater characteristics.

Another study that likewise involved a pilot-scale MBR was conducted by de Silva et al. [22]. Conditions were maintained at steady state, although the aerated and anoxic periods in the system were alternated every 2 h (i.e., 2-h aerated period and 2-h anoxic period). The pilot-scale MBR was operated at an HRT of 17 h and an SRT of 20 d. Again, most of the parameter values for the model were taken from published works or computed stoichiometrically. Comparison between the performance data and model simulation showed that the model was able to accurately predict the concentrations of sludge and nitrogen species and also to capture general trends for the soluble COD in the effluent.

One advantage of the SMP model over ASMs is its capability to accurately model biomass in MBRs without the need for calibration using experimental data. Also, it involves less components and equations while still capturing key quantities. On the other hand, there is less ease in model application compared to the ASM family, which is presented in matrix format, and the model does not incorporate biological phosphorous removal.

2.1.3. ASM1-SMP hybrid model

Another model that incorporates the formation and degradation of SMP is the ASM1-SMP hybrid model developed by Lu et al. [9]. In this modified version of ASM1, the same definition for SMP is used as in the SMP model described above. The main concepts of ASM1 are preserved in the hybrid model, but a few changes were made to include the fate of SMP. A schematic of the model that depicts these changes is provided in Fig. 5. UAPs are released in the metabolic processes of autotrophs and heterotrophs, and heterotrophs can reutilize UAPs for their growth. In addition to inert material and soluble substrates, the decay processes of the organisms produce BAPs, which can also be reused for heterotrophic growth. These changes were incorporated as follows. The component X_p, which denotes particulate products arising from biomass decay, was replaced with BAPs and UAPs. Process rates for aerobic and anoxic growths of heterotrophs by SMP consumption were added. Additionally, the decay rates of the two organisms were separated into two processes, i.e., one resulting in particulate formation and another resulting in BAP formation. The stoichiometric coefficients were adjusted accordingly with the inclusion of these rate processes. The model comprises 12 transient mass balance equations without alkalinity.

Experiments were carried out with a single completely mixed bioreactor that treated synthetic wastewater to test the validity of the AMS1-SMP hybrid model. The MBR was operated with aerobic and anoxic cycling of 60 min (30 min with aeration, 30 min without aeration) and 120 min (60 min with aeration, 60 min without aeration). Most original parameters of ASM1 were used, but the denitrification correction factor was enhanced to account for higher sludge concentrations in the system. Parameter values arising from the modification to include SMPs were determined by trial and error or obtained from references. The model simulation results showed good correspondence

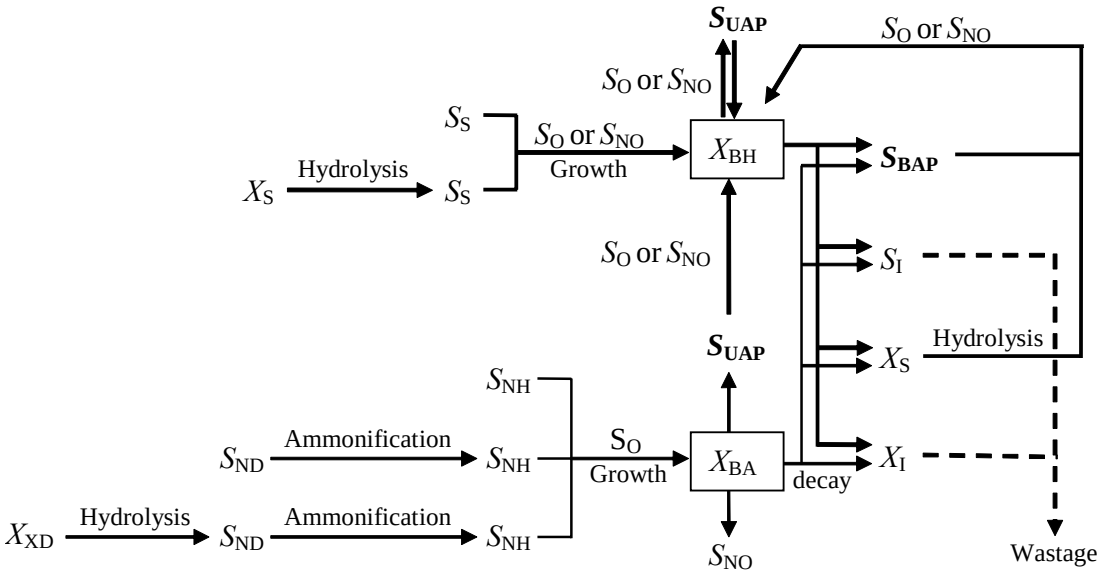

Fig. 5. Schematic of the ASM1-SMP hybrid model [9].

for soluble COD and soluble nitrogen concentrations under steady-state conditions. However, MLSS concentrations were significantly underestimated for both cycling conditions. This ASM1-SMP hybrid model is a first attempt at modifying the ASMs to model MBRs. Progress was made based on research that suggests the importance of the inclusion of SMP components for activated sludge with high SRTs. The incorporation of the SMP model into ASM1 takes advantage of some benefits of both models, although more work is needed to fine-tune the hybrid model.

2.2. Membrane fouling models

2.2.1. Empirical hydrodynamic model

To investigate the influence of hydrodynamic conditions on the mixed liquor crossflow velocity and the membrane fouling rate in an MBR, 10 experiments were performed at varying suspended solid (SS) concentrations (X, 2–20 g/L), permeate fluxes (J, 4.5–27 L/m^2/h), and aeration intensities (U_{Gr}, 10–100 m^3/m^2/h) in an internal-loop airlift reactor [23]. The reactor is shown in Fig. 6. Air is supplied only in the riser zone of the reactor, which is separated from the down-comer sections by baffle plates. The air hold-up in the riser section generates a difference in the bulk density of the liquid, inducing circulation between the two zones. The crossflow velocity is an important parameter to consider in the impedance of sludge buildup on the membrane surface. Throughout each experiment, the up-flow velocity of the mixed liquor in the riser zone (U_{sr}, m/s) and the transmembrane pressure (ΔP, Pa) were monitored. The up-flow velocity was measured as an observable value of the actual crossflow velocity of the mixed liquor along the membrane surface. Note that the aeration intensity, U_{Gr}, is distinct from the mixed liquor crossflow velocity, U_{sr}. The former is a controlled parameter in the experiment, whereas the latter is a measured value that is influenced by controlled parameters. The transmembrane pressure was used to calculate the membrane fouling rate (K, m/h), defined as the rate of increasing membrane filtration resistance (i.e., $K = \mathrm{d}R/\mathrm{d}t$).

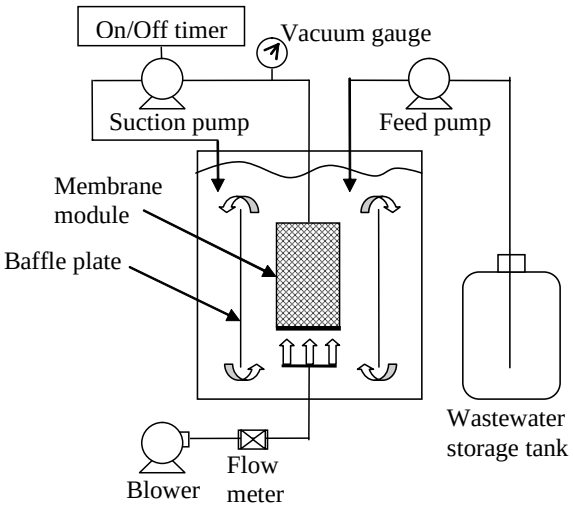

Fig. 6. Diagram of internal-loop-airlift reactor [23].

The following equation was used to compute filtration resistance (R, m^{-1}):

$$R = 3.6\times10^{9}\frac{\Delta P}{\eta J} \tag{4}$$

Here, η (mPa-s) is the viscosity of the permeate and is approximated as having the viscosity of tap water. The factor, 3.6×10^9, stems from using the units given in parentheses for each of the variables. Membrane resistance over time was plotted for each experiment, and the membrane fouling rate was obtained from the slope of the linear regression through the plot. Correlations were developed from the experimental data for the mixed liquor crossflow velocity and the membrane fouling rate as functions of the hydrodynamic parameters.

Aeration intensity, reactor structure, and fluid viscosity were the main factors influencing the mixed liquor crossflow velocity. The correlation for the crossflow velocity was assumed to fit the following power equation:

$$U_{sr} = f_1 U_{Lr}^{a}\mu^{b} \tag{5}$$

where U_{Lr} (m/s) is the crossflow velocity of tap water, μ is the mixed liquor viscosity (mPa-s), and f_1, a, and b are constants. U_{Lr} was found by measuring the up-flow velocity of tap water in the reactor. The parameter was used to capture the combined influence of aeration intensity and reactor structure. The reactor structure affects the sludge crossflow velocity but is not a directly quantifiable parameter. Multiple regression analysis was used to determine the value of the three constants. The relationship between sludge viscosity and SS concentration was established from experimental data as

$$\mu = 1.61e^{0.07X} \tag{6}$$

and was replaced in Eq. (5) to obtain U_{sr} in terms of X. The following was given as the final equation for the mixed liquor crossflow velocity:

$$U_{sr} = 1.311U_{Lr}^{1.226}e^{-0.0105X} \tag{7}$$

Key factors influencing the membrane fouling rate were aeration intensity (again captured by the tap water crossflow velocity to incorporate the effect of the reactor structure), permeate flux, and SS concentration. The parameters were fitted to the following power equation:

$$K = f_2 U_{Lr}^{c} J^{d} X^{e} \tag{8}$$

where f_2, c, d, and e are constants. The values of these constants, determined using the least squares method, are as follows: $f_2 = 8.933\times10^7$, $c = -3.047$, $d = 0.376$, and $e = 9.532$. Eqs. (7) and (8) are supplied to quantitatively characterize membrane fouling in an MBR.

The equations supplied by the hydrodynamic model explicitly show the correlation of various hydrodynamic parameters to two important factors: membrane fouling rate and mixed liquor crossflow velocity. The mixed liquor crossflow velocity is important because it gives insight into the impact of hydraulic conditions on membrane

fouling in terms of the retardation of sludge accumulation on the membrane surface. While the model is easy to use, it is too simple to capture the complicated phenomena on the membrane surface and so fails to account for many other conditions and operational parameters. Consequently, the model was unable to accurately reproduce the experimental results from which the model was calibrated for the membrane fouling rate. The calculated mixed liquor crossflow velocities corresponded well with the measured values, but it must be tested against a different set of experimental data to support its validity. In general, the model may be useful for illustrating hydrodynamic effects on membrane fouling, but it may not be suitable for operational and design purposes.

2.2.2. Fractal permeation model

A permeation model (based on fractal theory and Darcy's law) was developed by Meng et al. [24] to evaluate the permeability of cake formed from the microfiltration of activated sludge. The microstructure of a cake layer is usually disordered and complicated and, thus, cannot be described by traditional geometry. Fractal theory can be applied here to characterize the irregular object in terms of its average, self-similar properties. The authors first introduce a model to determine the pore area fractal dimension, D_s, of a cake layer:

$$B(\geq a) = S_c - A = C_0 \left(a\right)^{2-D_s} \tag{9}$$

where a is a threshold pore area, B is the total cake layer area (S_c) minus the sum (A) of all pore areas equal to or larger than a (i.e., $A = \Sigma a$), and C_0 is a constant. This model stems from a fractal model developed by Kaye et al. and Xu et al. [25, 26]. Meng et al. provide a procedure for physically determining the fractal dimension of a cake layer, which involves the use of an image analyzer to evaluate each pore area. Eq. (9) can be applied to calculate the values of B from several defined threshold values of a. The fractal dimension can then be computed from the slope of the straight line through the plot of ln B vs. ln a.

The permeability model was derived by modifying the Hagen–Poiseulle equation for flow rate through a tortuous capillary or pore [27]. The equation was rewritten in terms of the threshold pore area, a, rather than the pore diameter, λ, as follows

$$q(a) = \frac{G}{g}\frac{\Delta P}{L(a)}\frac{a^2}{\mu} \tag{10}$$

where G is the geometry factor for fluid flow through a pore (i.e., $\pi/128$ for circular pores), g is the shape factor where $a = g\lambda^2$, ΔP is the pressure gradient, $L(a)$ is the tortuous length of a pore, and μ is the dynamic viscosity. Straight pores were assumed in the cake layer, allowing the replacement of $L(a)$ by a constant, L_0. A unit flow rate was obtained by dividing Eq. (10) by a, and the infinitesimal flow rate dQ through an area dA was expressed as:

$$\mathrm{d}Q = -\frac{q(a)}{a}\mathrm{d}A = -\frac{G}{g^2}\frac{\Delta P}{L_0}\frac{a}{\mu}\mathrm{d}A \tag{11}$$

The portion of cake area, dA, was obtained by taking the derivative of Eq. (9) with respect to a:

$$\mathrm{d}A = -C_0\left(2 - D_s\right)a^{1-D_s}\mathrm{d}a \tag{12}$$

Substituting Eq. (12) into Eq. (11) and integrating Eq. (11) over the pore area distribution range ($a_{\min}$ to $a_{\max}$) gave

$$\begin{aligned} Q &= C_0\frac{G}{g^2}\frac{\Delta P}{L_0}\frac{1}{\mu}\left(2 - D_s\right)\int_{a_{\min}}^{a_{\max}} a^{2-D_s}\mathrm{d}a \\ &= \frac{G}{g^2}\frac{\Delta P}{L_0}\frac{1}{\mu}C_0\frac{2 - D_s}{3 - D_s}\left(a_{\max}^{3-D_s} - a_{\min}^{3-D_s}\right) \end{aligned} \tag{13}$$

which was reduced to

$$Q = \frac{G}{g^2}\frac{\Delta P}{L_0}\frac{1}{\mu}C_0\frac{2-D_s}{3-D_s}a_{\max}^{3-D_s} \quad (14)$$

by recognizing that the fractal dimension must be between 1 and 2, and a_{max} is much greater than a_{min} (i.e., $1 < D_s < 2$, so $3 - D_s > 1$ and $a_{max} \gg a_{min}$, so $a_{max}^{3-Ds} \gg a_{min}^{3-Ds}$). The expression for the flow rate, Q, in Eq. (14) was substituted into Darcy's law to obtain the following equation for the permeability of porous cake:

$$\kappa = \frac{\mu L_0 Q}{\Delta P A_t} = \frac{G}{g^2}C_0\frac{1}{A_t}\frac{2-D_s}{3-D_s}a_{\max}^{3-D_s} \quad (15)$$

Cake layer permeation factor, κ', was defined as

$$\kappa' = \frac{2-D_s}{3-D_s}a_{\max}^{3-D_s} \quad (16)$$

and was used to illustrate the validity of the model. A number of membrane fouling experiments were performed with varying activated sludge properties. The specific resistance of the cake layer, r_c, in each experiment was determined indirectly. The inverse of the specific cake resistance is equal to cake permeability; therefore, the plot of the permeation factor against $1/r_c$ should show high linearity if the model is valid. A correlation coefficient of 0.857 for the linear regression was observed. Based on this, the authors asserted that the model is reasonable to a certain degree and is theoretically valid.

The fractal permeation model provides a method for determining the permeability of cake buildup on a membrane surface. The model involves only a few parameters that are fairly easy to determine and does not require intensive computation to solve. However, the model was only indirectly validated; therefore more adequate verification is necessary to determine the model's applicability. Moreover, the model does not show how operational parameters and conditions affect cake resistance but primarily relies on the fractal dimension to capture different effects. Therefore, various parameters must be further correlated with the pore area fractal dimension (or permeation factor) to determine their effects on cake resistance.

2.2.3. Sectional resistance model

In a submerged MBR, coarse bubbles from aeration provide a cleaning mechanism for the immersed membrane modules by scouring the membrane surface. The shear force from aeration is unevenly distributed, resulting in non-uniform fouling. Li and Wang [28] applied a sectional approach to account for the uneven cake formation in determining total filtration resistance. They divided the membrane surface into equal fractional areas, $\Delta\varepsilon$, and calculated separate total resistances, R, for each section, which consist of inherent membrane resistance R_m, pore fouling resistance R_p, and resistances due to dynamic and stable sludge films, R_{sf} and R_{sc}, respectively. The total resistance in each section is then described as

$$R = R_m + R_p + R_{sf} + R_{sc} \quad (17)$$

The pore fouling resistance, R_p, is proportional to the amount of permeate produced and is given by

$$R_p = r_p \sum J\theta_f \quad (18)$$

where r_p is the specific pore fouling resistance, J is the permeate flux, and θ_f is the filtration period of an operational cycle. R_{sf} is the product of the specific resistance of the biomass in the dynamic film, r_{sf}, and the mass of the dynamic sludge film, M_{sf} (i.e., $R_{sf} = r_{sf}M_{sf}$). Likewise, R_{sc}, is equal to the product of the specific resistance of the sludge cake layer, r_{sc}, and the mass of biomass accumulated on the membrane surface, M_{sc} (i.e., $R_{sc} = r_{sc}M_{sc}$).

The mass of the sludge in the dynamic film

can be determined from the following equation during the filtration period:

$$\frac{dM_{sf}}{dt} = \frac{24CJ^2}{24J + C_d d_p G} - \frac{\beta(1-\alpha)GM_{sf}^2}{\gamma V_f t + M_{sf}} \quad (19)$$

The first and second terms of Eq. (19) represent the rate of attachment and detachment, respectively. The attachment rate was derived by considering the opposing forces (i.e., the drag force that leads to attachment and a lift force caused by turbulence) acting on a particle as it approaches the membrane. The probability of the deposition of particles on the membrane surface is given by the attachment force divided by the sum of the two forces. Multiplying this probability by the mass flux (the sludge concentration ´ the permeate flux) gives the rate of attachment. Here, C is the sludge concentration, J is the local permeate flux in the membrane section, C_d is the coefficient of the lifting force of a sludge particle of diameter d_p, and G is the shear intensity on the section of the membrane surface. The detachment rate was assumed to follow a first-order kinetic process, i.e., $(dM_{sf}/dt)_d = -K_d M_{sf}$. The rate coefficient, K_d, was thought to vary with the mass of the sludge film. It increases with M_{sf} and reaches a maximum with large values of M_{sf} so that a Monod-type equation, $K_d = \kappa_r M_{sf}/(\kappa_s + M_{sf})$, is proposed. Expressions were assumed for the maximum rate constant, κ_r, and half-saturation constant, κ_s. In the detachment rate expression, β is the erosion rate coefficient of the dynamic sludge, α is the stickiness of biomass particles, γ is the compression coefficient for dynamic sludge, V_f is water production within the filtration period of the operation cycle, and t is the filtration time. During the cleaning period when no attachment occurs, the rate of detachment is described as

$$\frac{dM_{sf}}{dt} = -\frac{\beta(1-\alpha)GM_{sf}^2}{0.1\gamma V_f \theta_f + M_{sf}} \quad (20)$$

The factor 0.1 in the denominator arises from the presumption that the compression coefficient during the cleaning period is reduced by a tenth of its original value. The remaining sludge after cleaning, ΔM_{sc}, adds to the stable sludge cake layer.

For the shear intensity, G, at each section, the following shear profile is assumed:

$$\frac{G}{G_0} = \begin{cases} \frac{1}{10} + \frac{9}{20}\left[1 + \sin\frac{(2\varepsilon_i - \varepsilon_a)\pi}{2\varepsilon_a}\right] & \varepsilon_i < \varepsilon_a \\ 1 & \varepsilon_i \geq \varepsilon_a \end{cases} \quad (21)$$

where G_0 is the apparent shear intensity of the fluid turbulence, ε_i is the accumulated membrane area fractions up to the i^{th} section, and ε_a is the sectional area of membrane surface with reduced shear intensity (where G/G_0 is less than 1).

The sectional resistance model was developed using a partially analytic approach. The model is intended to characterize membrane fouling in submerged MBRs where the membranes are subjected to shear flow from aeration. By dividing the membrane into sections and considering the resistance in each section, the model accounts for uneven cake formation stemming from varying shear distribution along the membrane surface. The advantages of this transient model are that it accounts for cleaning cycles and characterizes fouling development over time. Experiments were conducted using a submerged MBR, which filtered glucose-based synthetic wastewater with varying sludge concentrations, filtration fluxes, and aeration intensities. Comparison of the measured and computer-simulated trans-membrane pressure over MBR operation time revealed that the model is only able of capturing general trends and may not be suitable for applications requiring accurate modeling of membrane fouling phenomena.

2.3. Integrated models

The models reviewed in this section are not fully integrated, but only lightly coupled to characterize both biomass transformation processes and membrane fouling. They are a first step in MBR model integration, as no truly integrated models have been developed yet, to the best of our knowledge.

2.3.1. ASM1-SMP hybrid and resistance-in-series model

An integrated MBR model in which ASM1 was modified to include components for SMP and additional rate processes to describe SMP fate was presented by Lee et al. [10]. The resistance-in-series model was adapted to account for the influence of the biomass on membrane fouling. Much like the ASM1-SMP hybrid model presented by Lu et al. [9], four rate process expressions were added to ASM1. The model stochiometry was accordingly modified. The four processes are listed below.

- Aerobic growth from S_{SMP}:

$$\mu_{SMP} \frac{S_{O_2}}{K_{O_2} + S_{O_2}} \frac{S_{SMP}}{K_{SMP} + S_{SMP}} \frac{S_{NH_4}}{K_{NH_4} + S_{NH_4}} \frac{S_{ALK}}{K_{ALK} + S_{ALK}} X_H$$

- Anoxic growth from S_{SMP}:

$$\mu_{SMP} \eta_{NO_3} \frac{S_{SMP}}{K_{SMP} + S_{SMP}} \frac{K_{O_2}}{K_{O_2} + S_{O_2}} \frac{K_{NO_3}}{K_{NO_3} + S_{NO_3}} \frac{S_{NH_4}}{K_{NH_4} + S_{NH_4}} \frac{S_{ALK}}{K_{ALK} + S_{ALK}} X_H$$

- Lysis of heterotrophic organisms producing S_{SMP}: $b_{H,SMP} X_H$
- Lysis of autotrophic organisms producing S_{SMP}: $b_{A,SMP} X_A$

This model incorporates the influence of alkalinity and ammonia concentrations on heterotrophic growth rate into the additional process rate expressions. Note that the previously described ASM1-SMP hybrid model does not consider alkalinity and removes ammonia concentration limitations on the growth rates of heterotrophs.

To model membrane fouling, the following equation for total filtration resistance, R, was supplied:

$$R = R_m + m\alpha \tag{22}$$

where

$$m = k_m \frac{V_p X_{TSS}}{A} \tag{23}$$

Here, R_m is the membrane resistance, α is the specific resistance, k_m is a coefficient ranging from 0 to 1 to reflect crossflow filtration effects (e.g. $k_m = 1$ for dead-end filtration), V_p is the permeate volume, X_{TSS} is the concentration of total suspended solids (TSS) in the biomass, and A is the membrane surface area. SMP was assumed not to contribute to the membrane resistance since its concentration was thought to be negligible compared to the TSS concentration.

The resistance model given here involves few parameters for predicting total resistance on the membrane surface. The parameter values can be easily determined, and total resistance is simple to calculate. However, both the biomass kinetics and resistance models have not been validated, and the applicability of the models is unknown.

2.3.2. ASM3 and resistance-in-series model

In the study by Wintgens et al. [11], a model was introduced to describe the filtration performance of submerged capillary hollow fiber modules in an MBR. The model was combined with ASM3 to include characterization of the biologi-

cal treatment process. It was acknowledged that extra-cellular polymeric substances (EPS) produced by the microorganisms can hamper membrane performance, but no modifications were made to ASM3 to quantify this component.

In the model, permeate flux was given as

$$F = \frac{\Delta p_{\mathrm{TM}}}{\eta_P \left(R_M + R_C + R_F \right)} \tag{24}$$

where

$$\Delta p_{\mathrm{TM}} = p_{\mathrm{hydro}} + p_{\mathrm{pump}} - \Delta p_{ax} \tag{25}$$

The effective transmembrane pressure difference, Δp_{TM}, is the sum of the hydrostatic pressure, p_{hydro}, and the suction pressure, p_{pump}, minus the pressure loss from permeate flow along the hollow fibers, Δp_{ax}. Total resistance is the sum of membrane resistance, R_M, cake resistance, R_C, and fouling resistance R_F. Cake resistance is given by

$$R_C = k_C c_M \tag{26}$$

where k_C is the cake layer model parameter and c_M is the concentration at the membrane surface, which is described as

$$c_M = c_b e^{F(t)/k_P} \tag{27}$$

where c_b is bulk concentration, $F(t)$ is the transmembrane flux, k_F is the local mass transfer coefficient. The expression used for k_P is

$$k_P = \frac{\tau_W d_C}{\eta_F} \tag{28}$$

where τ_W is the mean wall shear stress, d_C is characteristic particle diameter, and η_F is viscosity of the activated sludge. The fouling resistance was given as

$$R_F = S_F \left(1 - e^{-k_F \int_0^t F(t) dt} \right) \tag{29}$$

where S_F and k_F are model parameters for fouling saturation and accumulated fouling, respectively, and $\int_0^t F(t)\mathrm{d}t$ is the total permeate volume per membrane area produced between two chemical cleanings. The final form of the permeate flux has an implicit expression:

$$F(t) = \frac{p_{hydro} + p_{pump} + \Delta p_{ax}}{\eta_P \left(R_M + k_C c_b e^{F(t)/k_P} + S_F \left(1 - e^{-k_F \int_0^t F(t)\mathrm{d}t} \right) \right)} \tag{30}$$

This model is based on the resistance-in-series model and was developed to describe the filtration performance of submerged capillary hollow fiber modules in an MBR. Like the sectional resistance model, this model accounts for cleaning cycles and incorporates time dependency to provide a continuous fouling profile. The model was tested against operational data from a full-scale MBR with two external filtration units. Data from the first unit were used to set model parameters by curve-fitting using the least-square-error method. Simulation results from the calibrated model were then compared with data from the second filtration unit. Except for the initial period of operation, the computed permeability over time corresponded well with measured data. The model was also validated with experimental data from a pilot MBR with submerged capillary hollow fiber membranes [29]. The simulation results for permeability evolution over time matched well the data from the pilot plant except for a major deviation at the end of the considered period. The deviation was explained by a drop in the organic load of the influent, a factor which was not considered in the simulation.

3. Concluding remarks

A mini-review of modeling studies on the application of MBR for the treatment of municipal wastewaters was conducted to assess current MBR

modeling efforts. Models describing biomass kinetics in an MBR include the ASM model family, the SMP model, and the ASM1-SMP hybrid model. The ASMs were developed to model the activated sludge process, and their ability to accurately describe the MBR process has not been verified by in-depth experiments.

Research suggests that SMPs are important components in describing biomass kinetics due to high SRTs in MBR systems. Accordingly, the SMP model demonstrated the capability of characterizing the biomass with a reasonable to high degree of accuracy. Also, a modified version of ASM1 that incorporates SMPs demonstrated fairly reasonable accuracy in quantifying COD and soluble nitrogen concentrations but underestimated MLSS concentrations. Further testing is needed to aid in model development.

Models describing membrane fouling include the empirical hydrodynamic model, fractal permeation model, sectional resistance model, and the two resistance-in-series models that were presented as a part of integrated models. The empirical hydrodynamic model is too simple to describe the membrane fouling phenomenon, and the sectional resistance model lacks accuracy. Both the fractal permeation model and resistance-in-series model by Lee et al. [10] provide good scientific insight, but specific experimental verification is necessary for general use of the models. The resistance-in-series model developed by Winitgens et al. [11] shows the most promise, as it is fairly accurate, accounts for cleaning cycles, and can predict permeability changes over time. Further tests are needed to determine whether the model requires calibration or if the model parameters are applicable to other MBR systems.

For any given wastewater treatment system, primary concerns are the effluent quality that the system is able to achieve and the investment and operating costs required for the system. The system must be able to treat the water to meet water quality standards as set forth by regulatory agencies, and it must, simultaneously, be economical. Therefore, model development should center on components for which water quality standards have been set and on parameters which are strongly correlated to cost. A few key model components and parameters for MBRs are given here.

Permeate flux and transmembrane pressure are directly related to cost. These two parameters are correlated by permeate viscosity and total resistance. The ability to quantify individual resistance (i.e., resistance from cake formation and adsorptive fouling) as a function of the various influencing parameters is important in determining which parameters have the greatest influence on fouling and for designing and optimizing the system to achieve an economical balance between production and applied pressure. Parameters that affect fouling include sludge concentration, shear rate, concentration of pore-blocking and membrane adsorptive materials in the feed, and membrane material properties.

MBRs typically operate at higher biomass concentrations than conventional biological treatment processes. The advantage that this provides is increased volumetric loading and less sludge production, which in turn lowers capital investment costs for civil works and reduces sludge disposal costs. Conversely, higher biomass concentrations can adversely affect membrane performance, necessitating increased membrane area to maintain permeate flow rate and, thus, increase investment costs. Biomass concentration also influences energy costs. A reduced oxygen transfer rate is associated with higher biomass concentrations, so energy cost for aeration increases accordingly. Additionally, higher sludge viscosity, with respect to greater biomass concentration, requires a larger applied pressure to achieve a certain permeate production goal. Determining the relationship between biomass concentration and other parameters can aid in identifying an optimal biomass concentration for operation, which can lead to significant economical savings.

Aeration accounts for a significant portion of energy costs in the operation of MBR systems.

Thus, optimizing the oxygen supply can favorably affect operating costs. Determining the dissolved oxygen requirement and the conditions to supply the optimal amount at a high transfer rate can reduce wasting oxygen. Some of the factors that influence the oxygen transfer rate include the MLSS concentration, the mechanical configuration of MBR, the type of bubbles used (fine or coarse), and the specific air flow rate. The oxygen requirement depends on the constituents in the wastewater, biomass concentration, and biomass growth rates.

It is important to include carbon and nutrient (nitrogen and phosphorous components) concentrations in MBR models, given that the bioreactors process performance is characterized by those components. COD, BOD, ammonia/ammonium, nitrate/nitrite, and orthophosphate concentrations in the effluent should be captured by MBR models. The respective concentrations of these components are affected by the concentration of the various types of organisms influencing the removal of certain components, growth rates of these organisms, and concentration of oxygen in the system.

SMPs comprise a major portion of the organic matter in effluents from biological treatment processes. It is crucial to quantify and also minimize SMPs in the effluent because they are possible precursors to trihalomethane and other disinfection by-products, competitively adsorb on activated carbon surfaces, and potentially lead to biological growth in distribution systems. Additionally, EPS, which is a form of SMP that surrounds the surfaces of microorganisms, contributes to membrane fouling, especially when the microorganisms form specific biofilms on the membrane surfaces. Factors that influences the formation of SMP (and EPS) include biomass concentration, loading rates, and sludge age.

Several of the existing models, particularly the ASMs, require validation to determine their applicability for modeling the MBR process and to evaluate whether they can serve as a base for future MBR model development. Membrane fouling in MBRs is affected by the biotransformation processes in the system, so the integration of biomass kinetics and membrane fouling models is essential for future modeling. Moreover, examination of alternative empirical modeling approaches, such as the application of artificial neural networks, is worthwhile to make a rigorous link between inputs and outputs of MBR systems and to find phenomenological interrelationships among components and parameters.

The main purpose of this review is to organize core ideas of current MBR studies by selecting key publications, to assess the state-of-the-art MBR modeling efforts, and to propose future direction for MBR simulation research in pursuit of a global optimization for design criteria, operation protocol, and cost evaluation. We hope this review contributes to reassessment of the current predictability of MBR processes and opens directions for developing fundamental mechanisms that rigorously govern MBR performance.

Acknowledgement

This work was supported by the U.S. Geological Survey, through the Water Resources Research Center, University of Hawaii at Manoa, Honolulu, and by Saehan Industries, Korea. This is contributed paper CP-2006-00 of the Water Resource Research Center.

References

[1] C.W. Smith, D. Gregorio and R.M. Taleott. The use of ultrafiltration membrane for activated sludge separation, Presented at the 24th Annual Purdue Industrial Waste Conference, 1969, pp. 1300–1310.

[2] W. Yang, N. Cicek and J. Ilg, State-of-the-art of membrane bioreactors: Worldwide research and commercial applications in North America, J. Membr. Sci., 270 (2006) 201–211.

[3] G. Tchobanoglous, F.L. Burton and H.D. Stensel, Wastewater Engineering: Treatment and Reuse, McGraw-Hill, Boston, 2004, pp. 854–865.

[4] J. Manem and R. Sanderson, Membrane bioreactors, water treatment membrane processes, J. Mallevialle, P.E. Odendaal and M.R. Wiesner, eds., McGraw-Hill, New York, 1996, pp. 17.1–17.31.
[5] M. Henze, C.P.L.J. Grady, W. Gujer, G.v.R. Marais and T. Matsuo, Activated Sludge Model No. 1, in IAWPRC Scientific and Technical Report No. 1, IAWPRC, London, 1987.
[6] M. Henze, W. Gujer, T. Mino, T. Matsuo, M.C. Wentzel and G.v.R. Marais, Activated Sludge Model No. 2, in IAWQ Scientific and Technical Report No. 3, IAWQ, London, 1995.
[7] M. Henze, W. Gujer, T. Mino, T. Matsuo, M.C. Wentzel, G.v.R. Marais and M.C.M. Van Loosdrecht, Activated sludge model No.2d, ASM2d, Wat. Sci. Technol., 39(1) (1999) 165–182.
[8] W. Gujer, M. Henze, T. Mino and M. van Loosdrecht, Activated sludge model No. 3, Wat. Sci. Technol., 39(1) (1999) 183–193.
[9] S.G. Lu, T. Imai, M. Ukita, M. Sekine, T. Higuchi and M. Fukagawa, A model for membrane bioreactor process based on the concept of formation and degradation of soluble microbial products, Wat. Res., 35(8) (2001) 2038–2048.
[10] Y. Lee, J. Cho, Y. Seo, J.W. Lee and K.-H. Ahn, Modeling of submerged membrane bioreactor process for wastewater treatment, Desalination, 146 (2002) 451–457.
[11] T. Wintgens, J. Rosen, T. Melin, C. Brepols, K. Drensla and N. Engelhardt, Modelling of a membrane bioreactor system for municipal wastewater treatment, J. Membr. Sci., 216 (2003) 55–65.
[12] M. Henze, W. Gujer, T. Mino and M. van Loosdrecht, Activated Sludge Models: ASM1, ASM2, ASM2d, and ASM3. Scientific and Technical Report Series. vol. 9, IWA Publishing, London, 2000.
[13] H.Y. Ng and S.W. Hermanowicz, Membrane bioreactor operation at short solids retention times: performance and biomass characteristics, Wat. Res., 39(6) (2005) 981–992.
[14] D.J. Barker and D.C. Stuckey, A review of soluble microbial products (SMP) in wastewater treatment systems, Wat. Res., 33(14) (1999) 3063–3082.
[15] X. Huang, R. Liu and Y. Qian, Behaviour of soluble microbial products in a membrane bioreactor, Process Biochem., 36(5) (2000) 401–406.
[16] H.-S. Shin and S.-T. Kang, Characteristics and fates of soluble microbial products in ceramic membrane bioreactor at various sludge retention times, Wat. Res., 37(1) (2003) 121–127.
[17] N. Park, B. Kwon, I.S. Kim and J. Cho, Biofouling potential of various NF membranes with respect to bacteria and their soluble microbial products (SMP): Characterizations, flux decline, and transport parameters, J. Membr. Sci., 258 (2005) 43–54.
[18] S. Rosenberger, C. Laabs, B. Lesjean, R. Gnirss, G. Amy, M. Jekel and J.C. Schrotter, Impact of colloidal and soluble organic material on membrane performance in membrane bioreactors for municipal wastewater treatment, Water Res., 40(4) (2006) 710–720.
[19] H.Y. Ng, T.W. Tan and S.L. Ong, Membrane fouling of submerged membrane bioreactors: Impact of mean cell residence time and the contributing factors, Environ. Sci. Technol., 40(8) (2006) 2706–2713.
[20] H. Furumai and B.E. Rittmann, Advanced modeling of mixed populations of heterotrophs and nitrifiers considering the formation and exchange of soluble microbial products, Wat. Sci. Technol., 26(3–4) (1992) 493–502.
[21] V. Urbain, B. Mobarry, V. de Silva, D.A. Stahl, B.E. Rittmann and J. Manem, Integration of performance, molecular biology and modeling to describe the activated sludge process, Wat. Sci. Technol., 37(4–5) (1998) 223–229.
[22] D.G.V. de Silva, V. Urbain, D.H. Abeysinghe and B.E. Rittmann, Advanced analysis of membrane-bioreactor performance with aerobic-anoxic cycling, Wat. Sci. Technol., 38(4–5) (1998) 505–512.
[23] R. Liu, X. Huang, Y.F. Sun and Y. Qian, Hydrodynamic effect on sludge accumulation over membrane surfaces in a submerged membrane bioreactor, Process Biochem., 39(2) (2003) 157–163.
[24] F. Meng, H. Zhang, Y. Li, X. Zhang and F. Yang, Application of fractal permeation model to investigate membrane fouling in membrane bioreactor, J. Membr. Sci., 262 (2005) 107–116.
[25] B.H. Kaye, A Random Walk Through Fractal Dimensions, VCH, New York, 1994, chap. 6.
[26] X.Y. Xu, J.R. Xu and Y. Kang, Dynamics of air pressure filtration and fractal filter cake constructure, J. Chem. Ind. Eng., 46 (1995) 8–14.
[27] B.M. Yu and W. Liu, Fractal analysis of permeabilities for porous media, AIChE J., 50(1) (2004) 46–57.
[28] X.-y. Li and X.-m. Wang, Modelling of membrane fouling in a submerged membrane bioreactor, J. Membr. Sci., (in press).
[29] S. Geissler, T. Wintgens, T. Melin, K. Vossenkaul and C. Kullmann, Modelling approaches for filtration processes with novel submerged capillary modules in membrane bioreactors for wastewater treatment, Desalination, 178 (2005) 125–134.